Published in final edited form as:
J Cell Physiol. 2010 August ; 224(2): 334–344. doi:10.1002/jcp.22103.

Agonist-evoked Ca^{2+} wave progression requires Ca^{2+} and IP_3

John G McCarron, **Susan Chalmers**, **Debbi MacMillan**, and **Marnie L. Olson**
Strathclyde Institute of Pharmacy & Biomedical Sciences, University of Strathclyde, John Arbuthnott Building, 27 Taylor Street, Glasgow G4 0NR, UK

Abstract

Smooth muscle responds to IP_3-generating agonists by producing Ca^{2+} waves. Here, the mechanism of wave progression has been investigated in voltage-clamped single smooth muscle cells using localized photolysis of caged IP_3 and the caged Ca^{2+} buffer diazo-2. Waves, evoked by the IP_3-generating agonist carbachol (CCh), initiated as a uniform rise in cytoplasmic Ca^{2+} concentration ($[Ca^{2+}]_c$) over a single though substantial length (~30 μm) of the cell. During regenerative propagation, the wave-front was about 1/3 the length (~9 μm) of the initiation site. The wave-front progressed at a relatively constant velocity although amplitude varied through the cell; differences in sensitivity to IP_3 may explain the amplitude changes. Ca^{2+} was required for IP_3-mediated wave progression to occur. Increasing the Ca^{2+} buffer capacity in a small (2 μm) region immediately in front of a CCh-evoked Ca^{2+} wave halted progression at the site. However, the wave front does not progress by Ca^{2+}-dependent positive feedback alone. In support, colliding $[Ca^{2+}]_c$ increases from locally-released IP_3 did not annihilate but approximately doubled in amplitude. This result suggests that local IP_3-evoked $[Ca^{2+}]_c$ increases diffused passively. Failure of local increases in IP_3 to evoke waves appears to arise from the restricted nature of the IP_3 increase. When IP_3 was elevated throughout the cell, a localized increase in Ca^{2+} now propagated as a wave. Together, these results suggest that waves initiate over a surprisingly large length of the cell and that both IP_3 and Ca^{2+} are required for active propagation of the wave front to occur.

Keywords

Smooth muscle; calcium signaling; Ca^{2+} waves

INTRODUCTION

Virtually every activity smooth muscle cells perform, including contraction, cell division, growth and cell death, are controlled by changes in the cytoplasmic Ca^{2+} concentration ($[Ca^{2+}]_c$). The cell's facility for creating complex spatiotemporal signals, characterized by concentrations of Ca^{2+} that, in some regions, differ from the cytoplasmic average value, contributes to the cell's ability to regulate various processes (McCarron et al., 2006; Rizzuto and Pozzan, 2006). Complex spatiotemporal Ca^{2+} signals may be generated by entry of the ion from outside the cell across the plasma membrane and by release from the internal store. Voltage-dependent Ca^{2+} channels in the plasma membrane allow Ca^{2+} influx, while IP_3 receptors (IP_3R) and ryanodine receptors (RyR) permit release from the internal Ca^{2+} store (the sarcoplasmic reticulum; SR)(Chalmers et al., 2007).

Correspondence to: J.G. McCarron, Strathclyde Institute of Pharmacy and Biomedical Sciences, University of Strathclyde, John Arbuthnott Building, 27 Taylor Street, Glasgow G4 0NR, UK. Tel. +44 141 548 4119. Fax. +44 141 552 2562. john.mccarron@strath.ac.uk.

Europe PMC Funders Author Manuscripts

An increase in $[Ca^{2+}]_c$ arising from the generation of IP_3 initiates at discrete sites in the cell as localized transient rises (Bootman et al., 1997; Yao et al., 1995) to provide a short range intracellular signaling system and may activate nearby effectors. The limited range of the signal is accomplished, in part, by Ca^{2+} buffers and sequestration which each restrict the distance the ion can carry a signal within the cytoplasm i.e. the 'excitability' of the SR appears to be controlled. Longer range signaling requires the local rises to be transmitted through the cell. A common form of transmission occurs when local rises progress as a travelling spatial gradient of the ion (Ca^{2+} waves). Such transmission occurs when short range signals appear to interact and coalesce so that the cytoplasm and SR become 'excitable' and regenerative propagation of the Ca^{2+} wave occurs to spread information within and between cells (Balemba et al., 2006; Bootman et al., 1997; Lansley and Sanderson, 1999). The mechanisms underlying Ca^{2+} waves, like action potentials, differ in various cell types (Bai et al., 2009; Balemba et al., 2006; Jaggar and Nelson, 2000; Ruehlmann et al., 2000; Sergeant et al., 2009; White and McGeown, 2002).

In each of short and long range signals, information is encoded in the frequency of the Ca^{2+} change. For example, smooth muscle contraction is regulated by the frequency of agonist induced Ca^{2+} waves (Bai and Sanderson, 2006; Iino et al., 1994; Kasai et al., 1997; Perez and Sanderson, 2005). The frequency of Ca^{2+} waves and oscillations may also regulate gene expression patterns and protein kinase activities (De Koninck and Schulman, 1998; Dolmetsch et al., 1998; Li et al., 1998). Thus it is important to understand the mechanism which underlies wave formation and progression.

Two main mechanisms for the propagation of Ca^{2+} waves have been proposed, each involve those receptors present on the SR which govern Ca^{2+} release i.e. RyR and IP_3R. In the first proposal RyR acts as the major channel responsible for Ca^{2+} wave propagation (Boittin et al., 1999; Goldbeter et al., 1990). Following IP_3-generating agonist activity at the sarcolemma, a priming release of Ca^{2+} via IP_3R initiates Ca^{2+}-induced Ca^{2+} release (CICR) at RyR. Thereafter, the wave proceeds independently of IP_3 and Ca^{2+} release occurs exclusively by RyR activity (Balemba et al., 2006; Boittin et al., 1999; Ruehlmann et al., 2000; Straub et al., 2000). The second proposal for wave propagation relies exclusively on the activity of IP_3R (Bai et al., 2009; Lamont and Wier, 2004; McCarron et al., 2004). IP_3 initially opens and sensitizes the channel to positive feedback by cytoplasmic Ca^{2+}. After a priming release of Ca^{2+} by IP_3, IP_3R may also serve as sites for Ca^{2+}-induced Ca^{2+} release (CICR), being opened by released Ca^{2+} in a positive feedback process (Bootman et al., 1997; Iino and Tsukioka, 1994; Meyer et al., 1988).

In each proposal for wave progression, there is a requirement for positive feedback to evoke the regenerative response required to progress the wave. Ca^{2+}, it is proposed, may provide the positive feedback via the Ca^{2+} dependencies of the release channels (Berridge, 1997). Although a generally accepted hypothesis, direct experimental support which demonstrates the nature of the feedback required for IP_3-mediated wave progression is absent. In the case of IP_3R, support for a role of Ca^{2+} in wave progression appears to be derived largely from experiments which show that IP_3 and Ca^{2+} act synergistically to activate the receptor (Bezprozvanny et al., 1991; Finch et al., 1991; Iino, 1990). While these observations demonstrate release from IP_3R may be facilitated by Ca^{2+} they do not show that the ion provides the positive feedback required for sequential activation of IP_3R so that release progresses from site to site though the cell. RyR is activated by Ca^{2+} (Endo et al., 1970) and may contribute to wave progression. However, the contribution of RyR to wave progression is unresolved and the Ca^{2+} concentration required to activate the channel may be higher than the changes which occur in the bulk cytoplasm during wave progression (reviewed in McCarron et al., 2003).

In the present study localized (2 μm) photolysis of caged IP_3 and diazo-2 (a caged Ca^{2+} buffer) has permitted rapid and reproducible increases in IP_3 and $[Ca^{2+}]_c$ or decreases in $[Ca^{2+}]_c$ respectively in subcellular compartments of intact cells and a more direct evaluation of the role of IP_3R in Ca^{2+} wave propagation to be made. This study has shown that the cytoplasm and SR are relatively inexcitable structures; when there is a confined increase in IP_3 concentration, the local increase in $[Ca^{2+}]_c$ produced remains restricted to the site of release and does not progress through the cell. Under conditions of cell-wide activation, Ca^{2+} waves in smooth muscle progress by sequential release of Ca^{2+} from the IP_3R triggered by Ca^{2+} itself and requiring IP_3.

MATERIALS AND METHODS

Cell Isolation

Male guinea-pigs (300-500 g) were humanely killed by cervical dislocation followed by immediate exsanguination in accordance with the guidelines of the Animal (Scientific Procedures) Act UK 1986. A segment of intact distal colon (~5 cm) was transferred to oxygenated (95% O_2 - 5% CO_2) physiological saline solution composed of (mM): NaCl (118.4), $NaHCO_3$(25), KCl (4.7), NaH_2PO_4 (1.13), $MgCl_2$ (1.3), $CaCl_2$ (2.7), and glucose (11) (pH 7.4). Following removal of the mucosa from the tissue, single smooth muscle cells were enzymatically dissociated (McCarron and Muir, 1999).

Cells were stored at 4 °C and used within 24 hours of cell isolation. All experiments were carried out at room temperature (20 ± 2 °C).

Electrophysiology

Membrane currents were measured using conventional tight seal whole-cell recording methods previously described (Chalmers and McCarron, 2008; Kamishima and McCarron, 1998; MacMillan et al., 2005b). The normal extracellular solution contained (mM): Na glutamate (80), NaCl (40), tetraethylammonium chloride (TEA) (20), $MgCl_2$ (1.1), $CaCl_2$ (3), Hepes (10) and glucose (30) (pH 7.4 with NaOH). A Ca^{2+}-free extracellular solution had the same composition except there was no added Ca^{2+} and it additionally contained EGTA (10 mM). The pipette solution contained (mM): Cs_2SO_4 (85), CsCl (20), $MgCl_2$ (1), Hepes (30), MgATP (3), pyruvic acid (2.5), malic acid (2.5), NaH_2PO_4 (1), creatine phosphate (5) and guanosine phosphate (0.5). In some experiments (described in the Results) either caged IP_3 (50 μM) or the caged Ca^{2+} buffer diazo-2 (400 μM) were included in the patch pipette filling solution. Whole-cell currents were measured using an Axopatch 200B (Axon Instruments, Union City, CA, USA), low-pass filtered at 500 Hz, digitally sampled at 1.5 kHz using a Digidata interface and pClamp (version 10; Axon Instruments) and stored for analysis (McCarron and Olson, 2008).

Imaging

Cells were loaded with fluo-5F acetoxymethylester (AM) (5 μM) together with wortmannin (10 μM; to prevent contraction) for at least 20 minutes prior to the beginning of the experiment (McCarron et al., 2009).

Wide-field epi-fluorescence excitation illumination was provided by a monochomator (PTI Inc, West Sussex, UK) to give 490 nm (bandpass 5 nm) coupled via a liquid light guide to a Nikon TE2000U microscope (Nikon UK, Surrey England). Fluorescence emission was collected by the objective lens (×40, NA 1.3) and transmitted to a cooled, back-illuminated, frame transfer CCD camera with on-chip electron multiplication (Cascade 512B; Photometrics Tuscan, AZ. USA) controlled by EasyRatio pro software (1.2.1.87, PTI) illumination at a frequency of ~30 Hz unless otherwise indicated (McCarron et al., 2009).

Photolysis of either caged-IP_3 or diazo-2 was achieved using a frequency tripled ND:Yag (wavelength 355 nm) laser attached directly to the microscope (Rapp Optoelektronic, Hamburg, Germany). The position of the photolysis site (~2 μm diameter) was computer controlled (Rapp Optoelektronic). The duration of the photolysis pulse was 5 ms and energy, measured at the objective, 100 μW.

Electrophysiological measurements and imaging data were synchronized by recording, on pClamp, a transistor transistor logic (TTL) output from the CCD camera, which reported both its frame capture and readout status together with the electrophysiological information. In some experiments, flash photolysis was coordinated with the occurrence of depolarization of the plasma membrane by using triggering TTL outputs which were timed using pClamp.

Data Analysis

[Ca^{2+}] images were analyzed using the program Metamorph 7.5 (Molecular Devices Ltd., Wokingham, U.K.). To compensate for variations in fluorescence across the imaging field e.g. from irregularities in focus of the smooth muscle cell, fluorescence signals were background subtracted and expressed as ratios (F/F_0 or $\Delta F/F_0$) of fluorescence counts (F) relative to baseline (control) values (taken as 1) before stimulation (F_0). The extent of the Ca^{2+} wave front was measured as the distance covered by wave front (full-width) at the half-maximum amplitude (FWHM) of the $[Ca^{2+}]_c$ rise.

Summarized results are expressed as mean ± SEM of n cells. A paired or unpaired Student's t-test was applied to the raw data as appropriate; $p<0.05$ was considered significant.

Drugs and Chemicals

Drugs were applied either by hydrostatic pressure ejection or addition to the extracellular solution as stated in the text. CCh was applied in a Ca^{2+}-free bath solution. Sub-threshold concentrations of CCh were achieved by withdrawing the puffer pipette from the cell (so increasing the diffusion pathway) and effectively reducing the concentration of CCh reaching the cell. This approach made it possible to quickly and easily titrate the CCh concentration to determine the sub-threshold value empirically in each cell. Concentrations in the text refer to the salts where appropriate. Fluo-5F AM was purchased from Invitrogen (Paisley, UK). All other reagents were purchased from Sigma (Poole, UK).

RESULTS

Depolarisation- and CCh-induced $[Ca^{2+}]_c$ changes

Depolarization (−70 mV to +10 mV) activated membrane currents and increased $[Ca^{2+}]_c$ approximately uniformly throughout the cell (Fig 1). Ca^{2+} release from the SR does not contribute to the depolarization-evoked $[Ca^{2+}]_c$ rise in this cell type (Bradley et al., 2002). The $[Ca^{2+}]_c$ increase evoked by the IP_3 -generating muscarinic agonist carbachol (CCh, 100 μM by pressure ejection), on the other hand, began usually in one region and progressed through the cell as a travelling spatial $[Ca^{2+}]_c$ gradient (i.e. a Ca^{2+} wave; Fig 1). CCh was applied in a Ca^{2+}-free bath solution to ensure the $[Ca^{2+}]_c$ rise arose solely from release from the SR. Active propagation appeared to be required for progression of the Ca^{2+} rise through the cell. In support, the velocity away from the initiating release site was relatively constant as the wave progressed through the cell (Fig 1; n=5) although may have appeared faster at the initiation site (see below).

While the CCh-evoked Ca^{2+} wave appeared to progress by active propagation, wave amplitude varied in different regions of the cell (Fig 1). One explanation is that the magnitude of response to IP_3 varies in different parts of the cell. Support for this proposal is

found in experiments which liberate IP_3 in small regions (2 μm) of the cell by localized photolysis of a caged form of the inositide (Fig 2). The amplitude of IP_3-evoked Ca^{2+} release was not constant through the cell (Fig 2). IP_3 released near the nucleus evoked a larger $[Ca^{2+}]_c$ rise (5.7 ± 2.4 $\Delta F/F_0$) than occurred in peripheral regions of the cell (2.1 ± 1.6 $\Delta F/F_0$ and 0.8 ± 0.4 $\Delta F/F_0$ the latter value was at the site closest to the patch pipette; n=4). Together these experiments suggest that CCh-evoked Ca^{2+} waves progress actively through the cell but with regional variations in amplitude of the Ca^{2+} response.

CCh-evoked Ca^{2+} waves required IP_3R activity; waves were blocked by the IP_3R antagonist 2-APB. In these experiments, in control, the $[Ca^{2+}]_c$ increase evoked by CCh was 1.24 ± 0.22 ($\Delta F/F_0$) which was significantly ($p<0.01$; n=5) reduced by 2-APB (100 μM) to 0.14 ± 0.04 ($\Delta F/F_0$)(not shown). 2-APB neither blocks RyR nor reduces the SR Ca^{2+} content in this cell type (McCarron et al., 2002). Previous findings also show the CCh-evoked Ca^{2+} rise to be blocked by heparin (McCarron et al., 2002).

Initiation of wave progression is more apparent when the wave front alone is shown (Fig 3). The active wave front, revealed by the forward difference of the $[Ca^{2+}]_c$ changes, was derived by sequential subtraction of the images (Fig 3). The results show that the wave initiated as an approximately uniform increase in $[Ca^{2+}]_c$ over a relatively large length of the cell (31 ± 4 μm, FWHM; n=4; Fig 3). The latter may have contributed to the apparently faster rate of wave progression which occurred at the initiation site (Fig 1). The $[Ca^{2+}]_c$ in the initiation site reached an amplitude of 1.7 ± 0.6 $\Delta F/F_0$ (n=4) before regenerative progression became evident. The duration of the $[Ca^{2+}]_c$ changes at the initiation site and those of the wave front were not different, each being ~200 ms. Interestingly, after progression began, the wave front was substantially smaller (8.8 ± 1.3 μm; FWHM) at 30 ± 7% of the length of the $[Ca^{2+}]_c$ change which occurred at the initiation site. The amplitude of the $[Ca^{2+}]_c$ change in the wave front was similar (2.3 ± 1.2 $\Delta F/F_0$) to the peak value measured at the initiation site.

Mechanisms of wave production

One method by which the IP_3-evoked Ca^{2+} wave front is proposed to propagate is via activation of RyR by CICR. To examine this, IP_3 was released by photolysis at two small regions (each ~2 μm in diameter) ~100 μm apart within the cell (Fig 4). The localized increases in $[Ca^{2+}]_c$ were measured at each of the photolysis sites and also at a region between the photolysis sites. Following IP_3 release an increase in $[Ca^{2+}]_c$ was measured (photolysis site 1, 3.14 ± 1.25 $\Delta F/F_0$; photolysis site 2, 2.95 ± 1.3 $\Delta F/F_0$; n=4). As $[Ca^{2+}]_c$ moved from the release site the amplitude declined and at a region between the two photolysis sites (~50 μm from each release site; region 3) was ~20% of peak values. After photolysis at site 1 $[Ca^{2+}]_c$ measured 0.73 ± 0.31 $\Delta F/F_0$ (~50 μm from each release site) while after photolysis at site 2, 0.64 ± 0.5 $\Delta F/F_0$ (~50 μm from each release site) (n=4).

The question arises, does any of the $[Ca^{2+}]_c$ increase measured away from the release site require active propagation via RyR? If RyR are progressing the wave, the SR acts as an ‘excitable’ membrane to propagate waves via a sequential positive feedback activation of RyR. A property of waves which propagate on an ‘excitable’ surface is that colliding wave fronts annihilate (Jouaville et al., 1995; Lechleiter et al., 1991; Lechleiter and Clapham, 1992). Whether or not colliding wave fronts annihilated was examined next by photolyzing IP_3 almost simultaneously (~2 ms apart) at the two sites and the $[Ca^{2+}]_c$ change measured at the site of wave front contact (Fig 4, region 3). Annihilation would be evident as the $[Ca^{2+}]_c$ amplitude at the point of contact remaining unchanged despite the site having received Ca^{2+} from two sources (i.e. both photolysis sites). On the other hand, passive diffusion of Ca^{2+} from each of the release sites, and absence of active propagation, would be revealed by an increased amplitude of $[Ca^{2+}]_c$ at the point of contact. The increased amplitude occurs from

a passive summation of the ion concentration received from each of the two sources. In the event, when IP_3 was released at the two sites, the $[Ca^{2+}]_c$ change at the wave front point of contact (Fig 4, region 3) approximately doubled in amplitude (1.35 ± 0.41 $\Delta F/F_0$; n=4; $p<0.05$; Fig 4C, green line). This result suggests that the $[Ca^{2+}]_c$ increase, generated by local photolysis of caged IP_3, had diffused passively along the cell and questions the importance of positive feedback at RyR in IP_3-evoked Ca^{2+} wave propagation.

Role of IP_3 in wave progression

While the IP_3-producing agonist CCh was effective, local (photolyzed) increases in IP_3 failed to produce a propagating Ca^{2+} wave (Fig 2 & 4). Failure could have been due to the increases in IP_3 being restricted to small areas within the cell, while wave generation required a cell-wide elevation in IP_3. The question of whether or not a localized intracellular increase in IP_3 could evoke a Ca^{2+} wave was addressed next by locally releasing IP_3 in the presence of a low concentration of CCh which, by itself, did not evoke Ca^{2+} release. The low concentrations of CCh were used to generate a global elevation in IP_3. Low concentrations of CCh were achieved by withdrawing the ejection pipette from the cell so increasing the diffusion pathway and effectively reducing the concentration of CCh reaching the cell (see Methods). Under these circumstances a localized increase in IP_3 successfully generated a propagating $[Ca^{2+}]_c$ wave (Fig 5).

The amplitude of the IP_3-evoked Ca^{2+} increase was reduced after exposure to the low concentration of CCh (Fig 5). A CCh-evoked slow leak of Ca^{2+} from the SR to reduce the SR Ca^{2+} content (balanced by increased activity of pumps on the plasma membrane) or inactivation of some IP_3R by either Ca^{2+} or IP_3 (Hajnoczky and Thomas, 1994; McCarron et al., 2004; Oancea and Meyer, 1996) itself may explain the reduced amplitude.

Activation of protein kinase C by sub-threshold CCh is unlikely to explain the progression of the IP_3-evoked Ca^{2+} increase as a wave. None of the PKC antagonists H-7 or inhibitory peptide (PKC19-36) or agonist indolactam significantly altered IP_3-evoked Ca^{2+} increases in this cell type (McCarron et al., 2002).

Role of Ca^{2+} in wave progression

The failure of a localized $[Ca^{2+}]_c$ rise, evoked by local release of IP_3, to propagate through the cell suggests Ca^{2+} alone cannot act as the stimulus in wave propagation. Had it done so the localized $[Ca^{2+}]_c$ rise following release of IP_3 would have generated a Ca^{2+} wave. The results presented in Fig 5 suggest that a global elevation in IP_3 is required for progression to occur, but the question arises does Ca^{2+} contribute to wave propagation? To address this question, a Ca^{2+} wave was initiated by CCh and the $[Ca^{2+}]_c$ changes which occurred along the line of progression attenuated by increasing the Ca^{2+} buffer capacity in a small, restricted region of the cell. If Ca^{2+} is required for progression then the wave will terminate at the site of increased buffering. On the other hand, if Ca^{2+} is not required for wave progression then, in the presence of the buffer, the wave will proceed undiminished beyond the site of increased buffering (although amplitude will be reduced at the site of increased buffering). The increase in buffer capacity was achieved by localized flash photolysis of a caged Ca^{2+} buffer (diazo-2).

Controls were first carried out to confirm the ability of diazo-2 to locally attenuate Ca^{2+} rises. To do this, the buffering produced by various concentrations (100 μM – 1 mM) of diazo-2 was examined on depolarization-evoked $[Ca^{2+}]_c$ increases. Diazo-2 (1 mM) increased the buffer capacity of the cell *in the absence of photolysis* presumably because of the presence of some free (uncaged) buffer in the compound. Lower diazo-2 concentrations (100 μM), *when photolyzed*, did not produce a significant change in Ca^{2+} buffering in the

present experimental conditions. Diazo-2 (400 μM) did not alter the buffer capacity of the cell in the absence of photolysis and produced an approximate doubling of the buffer power when release by localized flash photolysis. Fig 6 shows an example of localized photolysis of diazo-2 on depolarization-evoked $[Ca^{2+}]_c$ increases. In the experiment, depolarization (−70 mV to +10 mV; 100 ms) activated I_{Ca} and evoked approximately reproducible rises in $[Ca^{2+}]_c$ (Fig 6B). Next, the depolarization was repeated but, in this case, diazo-2 was photolyzed 100 ms before (Fig 6C) or 800 ms after (Fig 6D) the second depolarization. When photolyzed 100 ms before the depolarization the peak $[Ca^{2+}]_c$ was reduced by 50 ± 11% (1.4 ± 0.8 versus 0.62 ± 0.3 $\Delta F/F_0$; n=5). The increase in buffering was restricted to the site of photolysis and peak amplitude of the $[Ca^{2+}]_c$ change in nearby regions (20 μm away) was unchanged at 87 ± 3% of control values (1.5 ± 0.85 versus 1.4 ± 0.78 $\Delta F/F_0$; Fig 6C). When diazo-2 was photolyzed 800 ms after the depolarization, during the declining phase of the transient, $[Ca^{2+}]_c$ was reduced to 30 ± 9% of control (0.9 ± 0.5 versus 0.34 ± 0.25 $\Delta F/F_0$; n=5, Fig 6D). Again the increase in buffering was restricted to the site of photolysis and $[Ca^{2+}]_c$ in a nearby region (20 μm away) was unchanged at 96 ± 1.8% of control (0.94 ± 0.49 versus 0.93 ± 0.49 $\Delta F/F_0$; n=5). The experiments establish that localized photolysis of diazo-2 is effective in attenuating Ca^{2+} signals in small restricted regions of the cell.

In the next series of experiments diazo-2 (400 μM) was photolyzed at a small site just ahead of progression of a CCh-evoked Ca^{2+} wave. First CCh was applied to generate a wave and establish the approximate time the wave would occur. The latter value was required because photolysis in this series of experiments was triggered manually. $[Ca^{2+}]_c$ measurements were made at the site of wave origin (region 1) and at 20 μm intervals along the axis of the cell in which photolysis of diazo-2 occurred (regions 2 & 3; Fig 7). In controls, CCh evoked a Ca^{2+} wave which originated close to the nucleus (2.4 ± 0.4 $\Delta F/F_0$; n=4) and propagated from that site (2.5 ± 0.4 $\Delta F/F_0$ at site 2 and 1.4 ± 0.3 $\Delta F/F_0$ at site 3). Next, CCh was again applied to evoke a wave (2.5 ± 0.5 $\Delta F/F_0$ at site 1) but in this case the caged Ca^{2+} buffer diazo-2 (400 μm) was photolyzed at site 2 as wave approached this site. Photolysis of diazo-2 attenuated the Ca^{2+} rise at site 2 (1.4 ± 0.3 $\Delta F/F_0$) and substantially prolonged the time course of Ca^{2+} release as expected from the increase in Ca^{2+} buffer capacity at the site. Significantly the wave was arrested at that site and did not progress (Fig 7). The amplitude of the Ca^{2+} wave beyond the photolysis site (at site 3) was 17 ± 4% (0.2 ± 0.1 $\Delta F/F_0$; n=4) of control wave values measured at the same site. These results suggest that Ca^{2+}, in addition to global increases in IP_3, is required for agonist-evoked Ca^{2+} wave propagation to occur.

DISCUSSION

The results presented show spatial and temporal variations in smooth muscle Ca^{2+} signals. Depolarization-evoked $[Ca^{2+}]$ increases were approximately uniform in amplitude and time course throughout the cytoplasm. Presumably the distribution of Ca^{2+} channels across the plasma membrane, coupled with the slow diffusion, of the ion generates the relatively uniform change in the bulk cytoplasm (McCarron et al., 2009). In contrast to these uniform increases the $[Ca^{2+}]_c$ changes evoked by the IP_3-generating muscarinic agonist CCh began usually in one region of the cell and progressed from it by an active process (rather than by diffusion from a release site) as a travelling Ca^{2+} wave. In support of the active nature of its propagation, the velocity of wave progression away from the release site was relatively constant (~25 μM s^{-1}). If diffusion alone progressed the wave the velocity and amplitude would have declined from the release site. Interestingly, while the CCh-evoked $[Ca^{2+}]_c$ rise progressed through the cell as a wave, i.e. a non-uniform $[Ca^{2+}]_c$ increase, it began as a relatively uniform increase over a surprisingly large (~30 μm FWHM) length of the cell (i.e. ~20% of the full cell length) before wave propagation began. The uniform increase during initiation is consistent with asynchronous activation of IP_3R clusters at a region of the cell with either a higher sensitivity to IP_3 or rate of production of the inositide. Indeed there are

differences in sensitivity to IP_3 in different parts of the cell. Locally released IP_3, by photolysis of a caged form of the inositide in small regions of the cell, evoked larger $[Ca^{2+}]_c$ transients near the nucleus, where waves often began, than other regions of the cell. Wave progression presumably began when sufficient IP_3 was generated throughout the cell to enable CICR to occur at IP_3R and propagate from site to site through the cell. After initiation, while the wave progressed at the approximately constant velocity, the amplitude of the $[Ca^{2+}]_c$ rise varied in different regions of the cell. Again the differences in sensitivity to IP_3 in various parts of the SR may explain the different amplitudes. In this cell type, IP_3R are present on a single, luminally-continuous SR (McCarron and Olson, 2008).

An alternative proposal for wave progression is that a priming release of Ca^{2+} via IP_3R initiates CICR at RyR (Balemba et al., 2006; Boittin et al., 1999; Goldbeter et al., 1990; Ruehlmann et al., 2000) . Thereafter, the role of IP_3 and IP_3R ends and the wave proceeds exclusively by RyR activity. In this proposal the SR and cytoplasm act as 'excitable' media to propagate waves. A property of 'excitable' membranes and propagating waves is that colliding wave fronts annihilate (Lechleiter et al., 1991; Lechleiter and Clapham, 1992). To test that possibility, in the present study, IP_3 was liberated by photolysis nearly simultaneously in two parts of the cell ~100 μm apart and the $[Ca^{2+}]_c$ change at the point of contact from the two release events measured. The wave fronts did not annihilate but the amplitude of the $[Ca^{2+}]_c$ rise approximately doubled. The increase in amplitude arises from passive summation of ion concentrations from the two sources. The results suggest that following localized increases in IP_3, the SR in colonic smooth muscle did not act as an 'excitable' medium and, by implication, that Ca^{2+}, by itself, cannot explain wave progression. The results question the importance of RyR in IP_3-mediated Ca^{2+} wave propagation.

The proposed role of RyR in wave propagation has been derived principally from experiments which relied on drugs such as ryanodine, dantrolene, procaine and tetracaine claimed to be specific inhibitors of RyR. The drugs blocked Ca^{2+} waves leading to the conclusion that RyR are required to progress waves. However, some of these drugs may be less selective than previously assumed and may block IP_3R at concentrations thought selective for RyR (Bai et al., 2009; MacMillan et al., 2005a; Vites and Pappano, 1992). For example, in avian atria, ruthenium red inhibited the response to IP_3 by an action unrelated to RyR since the response to caffeine was potentiated (Vites and Pappano, 1992). Ryanodine, dantrolene, tetracaine and procaine also block IP_3-mediated Ca^{2+} release at concentrations which had been thought selective for RyR (Bai et al., 2009; MacMillan et al., 2005a). Dantrolene and tetracaine may block IP_3R directly (MacMillan et al., 2005a). In addition, relatively low concentrations (10 μM) of the RyR blocker tetracaine inhibited IP_3-mediated Ca^{2+} contraction by both decreasing IP_3 production and the Ca^{2+} sensitivity of the myofilaments in mouse airway smooth muscle (Bai et al., 2009). Inhibition of IP_3 production may be a mechanism common to local anaesthetics such as tetracaine and procaine (Bai et al., 2009; Hollmann et al., 2001). In the absence of precise information on the state of filling of the store, the complex action of ryanodine makes interpretation of its effects on IP_3-mediated responses difficult. Ryanodine may reduce IP_3-evoked Ca^{2+} release indirectly as a consequence of depletion of the SR of Ca^{2+} (Bai et al., 2009; Lamont and Wier, 2004; MacMillan et al., 2005a; McCarron et al., 2003; McCarron et al., 2002). These results question the exclusive use of drugs and pharmacological investigations to determine the mechanism of wave progression.

Contradictory evidence on the roles of RyR and IP_3R in wave propagation may stem also from experimental protocols which create abnormal 'store overload'. In 'store-overload' conditions RyR Ca^{2+} sensitivity is increased and this enables waves to be induced by RyR activity. In heart cells, for example, a high luminal $[Ca^{2+}]$ disables the self-limitation

process which operates on RyR to terminate release and promotes a 'feedforward' mechanism to open neighbouring RyR clusters and enables a Ca^{2+} rise to propagate through the cell as a wave (Cheng et al., 1996). The relevance of these to normal physiological functioning is unclear and RyR-mediated Ca^{2+} waves may be a pathological event in the heart (Eisner et al., 2009).

An elevated IP_3 concentration throughout the cell may be required for agonist-evoked waves to progress in smooth muscle. Thus while a localized release of IP_3 does not produce a propagating Ca^{2+} wave, when the cell was activated by a subthreshold concentration of CCh, to globally increase in the inositide, IP_3 released locally now generated a propagating wave. IP_3 may exert two effects to enable waves to occur. First, by activating Ca^{2+} release from an IP_3 R cluster, IP_3 generates a local increase in $[Ca^{2+}]_c$ (a Ca^{2+} 'puff'). Secondly, in the presence of activating levels of IP_3, elevations of $[Ca^{2+}]_c$ from Ca^{2+} released by one cluster may activate neighbouring clusters in a CICR-like process. The combination of an initiating Ca^{2+} release and CICR may act as the critical communication mechanism to generate cell wide Ca^{2+} signals (waves) from release events from individual IP_3R clusters (Berridge, 1997). In effect, IP_3 enables propagation by enhancing the excitability of the SR and cytoplasm. The IP_3 requirement for wave propagation will permit control over the sites in the cell where progression occurs; waves may only progress where IP_3R have been sensitized by IP_3.

In other types of smooth muscle, agonist-induced Ca^{2+} increases are also primarily mediated via IP_3R. In mouse small airway smooth muscle agonist-induced Ca^{2+} waves occurred via an IP_3-dependent mechanism without a requirement for RyR. In rat mesenteric arteries, agonist-evoked IP_3-mediated Ca^{2+} waves also progress without a contribution from RyR (Lamont and Wier, 2004). Norepinephrine-evoked Ca^{2+} waves (IP_3-mediated) persisted, in rat tail artery segments maintained in organ culture for days with a non-deactivating ryanodine analogue, while Ca^{2+} release evoked by caffeine was lost (Dreja et al., 2001). In CCh-stimulated (IP_3-mediated) uinea-pig taenia caeci, a wave of rapid regenerative Ca^{2+} release occurred as the local $[Ca^{2+}]_c$ reached a critical concentration (160 nM) (Iino et al., 1993). RyR did not contribute, and Ca^{2+}-dependent feedback control of IP_3R played a dominant role in the regenerative Ca^{2+} release (Iino et al., 1993). Each of these results, like those of the present study, suggests that RyR does not contribute to wave propagation.

While Ca^{2+} alone does not support wave propagation, the ion is nonetheless thought to be required for progression to occur perhaps by acting via the Ca^{2+}-sensitivity of IP_3R (Bai et al., 2009; Lamont and Wier, 2004; McCarron et al., 2004). IP_3-sensitive Ca^{2+} release sites are proposed to be coupled by the diffusion of Ca^{2+} from one release site to another to propagate the wave through the cell. Although assumed (Bai et al., 2009; Lamont and Wier, 2004; McCarron et al., 2004), direct experimental support for a contribution of Ca^{2+} to IP_3-mediated Ca^{2+} wave progression is absent. Indirect support for a role of Ca^{2+} is derived from several lines of experimental evidence. For example, IP_3 and Ca^{2+} act synergistically to activate IP_3R (Bezprozvanny et al., 1991; Finch et al., 1991; Iino, 1990). However, these experiments do not demonstrate that Ca^{2+} diffusing from one site activates neighbouring IP_3R clusters. Indirect support is also found in experiments which show that mitochondria to act as a 'firewall' to limit progression of Ca^{2+} waves in pancreatic acinar cells (Straub et al., 2000; Tinel et al., 1999) and atrial myocytes (Mackenzie et al., 2004). The localized Ca^{2+} buffering provided by mitochondria may restrict progression of Ca^{2+} waves (Mackenzie et al., 2004; Straub et al., 2000; Tinel et al., 1999). However, mitochondria may modulate Ca^{2+} wave progression by regulating the Ca^{2+} release channels via several mechanisms which are separate from their Ca^{2+} uptake facility e.g. free radical generation, ATP production and redox balance (Chalmers et al., 2007; Walsh et al., 2009). Increasing the Ca^{2+} buffer capacity of the cell prevents waves and saltatory propagation is replaced with a uniform

increase in $[Ca^{2+}]_c$ through the cell (McCarron et al., 2008). These latter experiments, however, do not distinguish between the requirement for Ca^{2+} in the initiation rather than progression of waves. In the present study, evidence for the role of Ca^{2+} in wave progression comes from experiments in which the Ca^{2+} buffer capacity of the cytoplasm was increased in small regions of the cell by locally photolyzing the caged Ca^{2+} chelator diazo-2. This local increase in buffer capacity of the cell halted waves at the site of photolysis. These results are consistent with a positive feedback effect of Ca^{2+} being a requirement for waves to propagate through the cell. The results do not distinguish between a requirement for Ca^{2+} to act on IP_3R either directly or indirectly, the latter via an increased local production of IP_3 (Young et al., 2003).

The present findings contribute to our understanding of the ways in which Ca^{2+} waves are generated and propagate in smooth muscle. The wave initiates as a relatively uniform increase in $[Ca^{2+}]_c$ and progresses by a CICR-like process acting on the IP_3R. The SR is normally a relatively inexcitable structure. The inexcitability of the SR will minimize propagation of false signals arising from the random activity of RyR or IP_3R and permit the cell to retain control over the progression of Ca^{2+} waves.

Acknowledgments

This work was funded by the Wellcome Trust (078054/Z/05/Z) and British Heart Foundation (PG/08/066); their support is gratefully acknowledged

LITERATURE CITED

Bai Y, Edelmann M, Sanderson MJ. The contribution of inositol 1,4,5-trisphosphate and ryanodine receptors to agonist-induced Ca^{2+} signaling of airway smooth muscle cells. Am J Physiol Lung Cell Mol Physiol. 2009; 297(2):L347–361. [PubMed: 19465516]

Bai Y, Sanderson MJ. Airway smooth muscle relaxation results from a reduction in the frequency of Ca^{2+} oscillations induced by a cAMP-mediated inhibition of the IP_3 receptor. Respir Res. 2006; 7:34. [PubMed: 16504084]

Balemba OB, Heppner TJ, Bonev AD, Nelson MT, Mawe GM. Calcium waves in intact guinea pig gallbladder smooth muscle cells. Am J Physiol Gastrointest Liver Physiol. 2006; 291:G717–727. [PubMed: 16710055]

Berridge MJ. Elementary and global aspects of calcium signalling. J Physiol. 1997; 499(Pt 2):291–306. [PubMed: 9080360]

Bezprozvanny I, Watras J, Ehrlich BE. Bell-shaped calcium-response curves of Ins(1,4,5)P3- and calcium-gated channels from endoplasmic reticulum of cerebellum. Nature. 1991; 351(6329):751–754. [PubMed: 1648178]

Boittin FX, Macrez N, Halet G, Mironneau J. Norepinephrine-induced Ca^{2+} waves depend on $InsP_3$ and ryanodine receptor activation in vascular myocytes. Am J Physiol. 1999; 277(1 Pt 1):C139–151. [PubMed: 10409117]

Bootman MD, Berridge MJ, Lipp P. Cooking with calcium: the recipes for composing global signals from elementary events. Cell. 1997; 91:367–373. [PubMed: 9363945]

Bradley KN, Flynn ER, Muir TC, McCarron JG. Ca^{2+} regulation in guinea-pig colonic smooth muscle: the role of the Na^{+}-Ca^{2+} exchanger and the sarcoplasmic reticulum. J Physiol. 2002; 538:465–482. [PubMed: 11790813]

Chalmers S, McCarron JG. The mitochondrial membrane potential and Ca^{2+} oscillations in smooth muscle. J Cell Sci. 2008; 121:75–85. [PubMed: 18073239]

Chalmers S, Olson ML, MacMillan D, Rainbow RD, McCarron JG. Ion channels in smooth muscle: regulation by the sarcoplasmic reticulum and mitochondria. Cell Calcium. 2007; 42(4-5):447–466. [PubMed: 17629940]

Cheng H, Lederer MR, Lederer WJ, Cannell MB. Calcium sparks and $[Ca^{2+}]_i$ waves in cardiac myocytes. Am J Physiol. 1996; 270(1 Pt 1):C148–159. [PubMed: 8772440]

De Koninck P, Schulman H. Sensitivity of CaM kinase II to the frequency of Ca^{2+} oscillations. Science. 1998; 279(5348):227–230. [PubMed: 9422695]

Dolmetsch RE, Xu K, Lewis RS. Calcium oscillations increase the efficiency and specificity of gene expression. Nature. 1998; 392(6679):933–936. [PubMed: 9582075]

Dreja K, Nordstrom I, Hellstrand P. Rat arterial smooth muscle devoid of ryanodine receptor function: effects on cellular Ca^{2+} handling. Br J Pharmacol. 2001; 132(8):1957–1966. [PubMed: 11309269]

Eisner DA, Kashimura T, O'Neill SC, Venetucci LA, Trafford AW. What role does modulation of the ryanodine receptor play in cardiac inotropy and arrhythmogenesis? J Mol Cell Cardiol. 2009; 46(4):474–481. [PubMed: 19150449]

Endo M, Tanaka M, Ogawa Y. Calcium induced release of calcium from the sarcoplasmic reticulum of skinned skeletal muscle fibres. Nature. 1970; 228(5266):34–36. [PubMed: 5456208]

Finch EA, Turner TJ, Goldin SM. Calcium as a coagonist of inositol 1,4,5-trisphosphate-induced calcium release. Science. 1991; 252(5004):443–446. [PubMed: 2017683]

Goldbeter A, Dupont G, Berridge MJ. Minimal model for signal-induced Ca^{2+} oscillations and for their frequency encoding through protein phosphorylation. Proc Natl Acad Sci U S A. 1990; 87(4): 1461–1465. [PubMed: 2304911]

Hajnoczky G, Thomas AP. The inositol trisphosphate calcium channel is inactivated by inositol trisphosphate. Nature. 1994; 370:474–477. [PubMed: 8047168]

Hollmann MW, Difazio CA, Durieux ME. Ca-signaling G-protein-coupled receptors: a new site of local anesthetic action? Reg Anesth Pain Med. 2001; 26(6):565–571. [PubMed: 11707797]

Iino M. Biphasic Ca^{2+} dependence of inositol 1,4,5-trisphosphate-induced Ca^{2+} release in smooth muscle cells of the guinea pig taenia caeci. J Gen Physiol. 1990; 95:1103–1122. [PubMed: 2373998]

Iino M, Kasai H, Yamazawa T. Visualization of neural control of intracellular Ca^{2+} concentration in single vascular smooth muscle cells in situ. Embo J. 1994; 13:5026–5031. [PubMed: 7957068]

Iino M, Tsukioka M. Feedback control of inositol trisphosphate signalling by calcium. Mol Cell Endocrinol. 1994; 98:141–146. [PubMed: 8143923]

Iino M, Yamazawa T, Miyashita Y, Endo M, Kasai H. Critical intracellular Ca^{2+} concentration for all-or-none Ca^{2+} spiking in single smooth muscle cells. EMBO J. 1993; 12(13):5287–5291. [PubMed: 8262071]

Jaggar JH, Nelson MT. Differential regulation of Ca^{2+} sparks and Ca^{2+} waves by UTP in rat cerebral artery smooth muscle cells. Am J Physiol Cell Physiol. 2000; 279(5):C1528–1539. [PubMed: 11029300]

Jouaville LS, Ichas F, Holmuhamedov EL, Camacho P, Lechleiter JD. Synchronization of calcium waves by mitochondrial substrates in Xenopus laevis oocytes. Nature. 1995; 377(6548):438–441. [PubMed: 7566122]

Kamishima T, McCarron JG. Ca^{2+} removal mechanisms in rat cerebral resistance size arteries. Biophys J. 1998; 75(4):1767–1773. [PubMed: 9746518]

Kasai Y, Yamazawa T, Sakurai T, Taketani Y, Iino M. Endothelium-dependent frequency modulation of Ca^{2+} signalling in individual vascular smooth muscle cells of the rat. J Physiol. 1997; 504(Pt 2):349–357. [PubMed: 9365909]

Lamont C, Wier WG. Different roles of ryanodine receptors and inositol (1,4,5)-trisphosphate receptors in adrenergically stimulated contractions of small arteries. Am J Physiol Heart Circ Physiol. 2004; 287(2):H617–625. [PubMed: 15072954]

Lansley AB, Sanderson MJ. Regulation of airway ciliary activity by Ca^{2+}: simultaneous measurement of beat frequency and intracellular Ca^{2+} Biophys J. 1999; 77(1):629–638. [PubMed: 10388787]

Lechleiter J, Girard S, Peralta E, Clapham D. Spiral calcium wave propagation and annihilation in Xenopus laevis oocytes. Science. 1991; 252(5002):123–126. [PubMed: 2011747]

Lechleiter JD, Clapham DE. Molecular mechanisms of intracellular calcium excitability in X. laevis oocytes. Cell. 1992; 69:283–294. [PubMed: 1568248]

Li W, Llopis J, Whitney M, Zlokarnik G, Tsien RY. Cell-permeant caged $InsP_3$ ester shows that Ca^{2+} spike frequency can optimize gene expression. Nature. 1998; 392(6679):936–941. [PubMed: 9582076]

Mackenzie L, Roderick HL, Berridge MJ, Conway SJ, Bootman MD. The spatial pattern of atrial cardiomyocyte calcium signalling modulates contraction. J Cell Sci. 2004; 117:6327–6337. [PubMed: 15561771]

MacMillan D, Chalmers S, Muir TC, McCarron JG. IP_3-mediated Ca^{2+} increases do not involve the ryanodine receptor, but ryanodine receptor antagonists reduce IP_3-mediated Ca^{2+} increases in guinea-pig colonic smooth muscle cells. J Physiol. 2005a; 569:533–544. [PubMed: 16195318]

MacMillan D, Currie S, Bradley KN, Muir TC, McCarron JG. In smooth muscle, FK506-binding protein modulates IP_3 receptor-evoked Ca^{2+} release by mTOR and calcineurin. J Cell Sci. 2005b; 118(Pt 23):5443–5451. [PubMed: 16278292]

McCarron JG, Bradley KN, MacMillan D, Muir TC. Sarcolemma agonist-induced interactions between $InsP_3$ and ryanodine receptors in Ca^{2+} oscillations and waves in smooth muscle. Biochem Soc Trans. 2003; 31(Pt 5):920–924. [PubMed: 14505449]

McCarron JG, Chalmers S, Bradley KN, Macmillan D, Muir TC. Ca^{2+} microdomains in smooth muscle. Cell Calcium. 2006; 40:461–493. [PubMed: 17069885]

McCarron JG, Chalmers S, Muir TC. "Quantal" Ca^{2+} release at the cytoplasmic aspect of the $Ins(1,4,5)P_3R$ channel in smooth muscle. J Cell Sci. 2008; 121(Pt 1):86–98. [PubMed: 18073237]

McCarron JG, Craig JW, Bradley KN, Muir TC. Agonist-induced phasic and tonic responses in smooth muscle are mediated by $InsP_3$. J Cell Sci. 2002; 115:2207–2218. [PubMed: 11973361]

McCarron JG, MacMillan D, Bradley KN, Chalmers S, Muir TC. Origin and mechanisms of Ca^{2+} waves in smooth muscle as revealed by localized photolysis of caged inositol 1,4,5-trisphosphate. J Biol Chem. 2004; 279:8417–8427. [PubMed: 14660609]

McCarron JG, Muir TC. Mitochondrial regulation of the cytosolic Ca^{2+} concentration and the $InsP_3$-sensitive Ca^{2+} store in guinea-pig colonic smooth muscle. J Physiol. 1999; 516:149–161. [PubMed: 10066930]

McCarron JG, Olson ML. A single luminally continuous sarcoplasmic reticulum with apparently separate Ca^{2+} stores in smooth muscle. J Biol Chem. 2008; 283(11):7206–7218. [PubMed: 18096697]

McCarron JG, Olson ML, Currie S, Wright AJ, Anderson KI, Girkin JM. Elevations of intracellular calcium reflect normal voltage-dependent behavior, and not constitutive activity, of voltage-dependent calcium channels in gastrointestinal and vascular smooth muscle. J Gen Physiol. 2009; 133(4):439–457. [PubMed: 19289573]

Meyer T, Holowka D, Stryer L. Highly cooperative opening of calcium channels by inositol 1,4,5-trisphosphate. Science. 1988; 240(4852):653–656. [PubMed: 2452482]

Oancea E, Meyer T. Reversible desensitization of inositol trisphosphate-induced calcium release provides a mechanism for repetitive calcium spikes. J Biol Chem. 1996; 271:17253–17260. [PubMed: 8663416]

Perez JF, Sanderson MJ. The frequency of calcium oscillations induced by 5-HT, ACH, and KCl determine the contraction of smooth muscle cells of intrapulmonary bronchioles. J Gen Physiol. 2005; 125(6):535–553. [PubMed: 15928401]

Rizzuto R, Pozzan T. Microdomains of intracellular Ca^{2+}: molecular determinants and functional consequences. Physiol Rev. 2006; 86:369–408. [PubMed: 16371601]

Ruehlmann DO, Lee CH, Poburko D, van Breemen C. Asynchronous Ca^{2+} waves in intact venous smooth muscle. Circ Res. 2000; 86(4):E72–79. [PubMed: 10700457]

Sergeant GP, Craven M, Hollywood MA, McHale NG, Thornbury KD. Spontaneous Ca^{2+} waves in rabbit corpus cavernosum: modulation by nitric oxide and cGMP. J Sex Med. 2009; 6(4):958–966. [PubMed: 19138373]

Straub SV, Giovannucci DR, Yule DI. Calcium wave propagation in pancreatic acinar cells: functional interaction of inositol 1,4,5-trisphosphate receptors, ryanodine receptors, and mitochondria. J Gen Physiol. 2000; 116(4):547–560. [PubMed: 11004204]

Tinel H, Cancela JM, Mogami H, Gerasimenko JV, Gerasimenko OV, Tepikin AV, Petersen OH. Active mitochondria surrounding the pancreatic acinar granule region prevent spreading of inositol trisphosphate-evoked local cytosolic Ca^{2+} signals. Embo J. 1999; 18(18):4999–5008. [PubMed: 10487752]

Vites AM, Pappano AJ. Ruthenium red selectively prevents Ins(1,4,5)P_3-but not caffeine-gated calcium release in avian atrium. Am J Physiol. 1992; 262(1 Pt 2):H268–277. [PubMed: 1370752]

Walsh C, Barrow S, Voronina S, Chvanov M, Petersen OH, Tepikin A. Modulation of calcium signalling by mitochondria. Biochim Biophys Acta. 2009; 1787(11):1374–1382. [PubMed: 19344663]

White C, McGeown JG. Carbachol triggers RyR-dependent Ca^{2+} release via activation of IP_3 receptors in isolated rat gastric myocytes. J Physiol. 2002; 542:725–733. [PubMed: 12154174]

Yao Y, Choi J, Parker I. Quantal puffs of intracellular Ca^{2+} evoked by inositol trisphosphate in Xenopus oocytes. J Physiol. 1995; 482(Pt 3):533–553. [PubMed: 7738847]

Young KW, Nash MS, Challiss RA, Nahorski SR. Role of Ca^{2+} feedback on single cell inositol 1,4,5-trisphosphate oscillations mediated by G-protein-coupled receptors. J Biol Chem. 2003; 278(23): 20753–20760. [PubMed: 12670945]

Europe PMC Funders Author Manuscripts

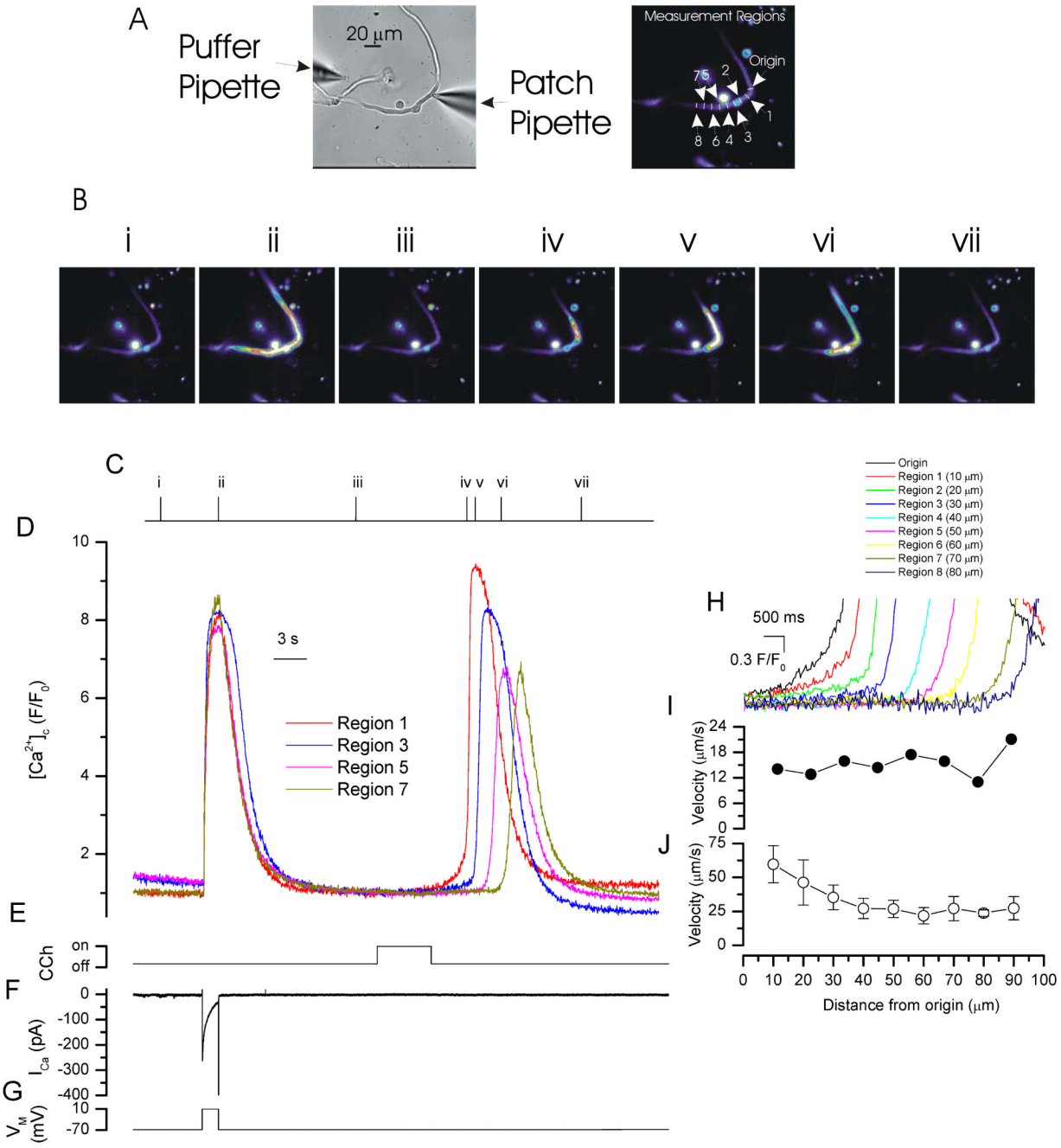

Figure 1. Depolarization and CCh-evoked increases in $[Ca^{2+}]_c$

Depolarization (−70 mV to +10 mV; G), activated a voltage-dependent Ca^{2+} current (I_{Ca}; F) to evoke a relatively uniform rise in $[Ca^{2+}]_c$ (B,D). In contrast, $[Ca^{2+}]_c$ increases in response to CCh began in one part of the cell and progressed from that site (B,D and expanded time base H). The $[Ca^{2+}]_c$ images (B) are derived from the time points indicated by the corresponding numerals in C. $[Ca^{2+}]_c$ changes in B are represented by colour; blue low and red/white high $[Ca^{2+}]_c$. Changes in the fluorescence ratio with time (D,H) are derived from 1 pixel lines ('origin' and regions 1-8 in A, right panel; drawn at a 3 pixel width to facilitate visualization). (A) left panel shows a bright field image of the cell; see also whole cell electrode (right side) and CCh containing puffer pipette (left side). The velocity of wave

progression is shown in I for the data presented (D,H) . Summarized velocity data is presented (J; n=5).

Europe PMC Funders Author Manuscripts

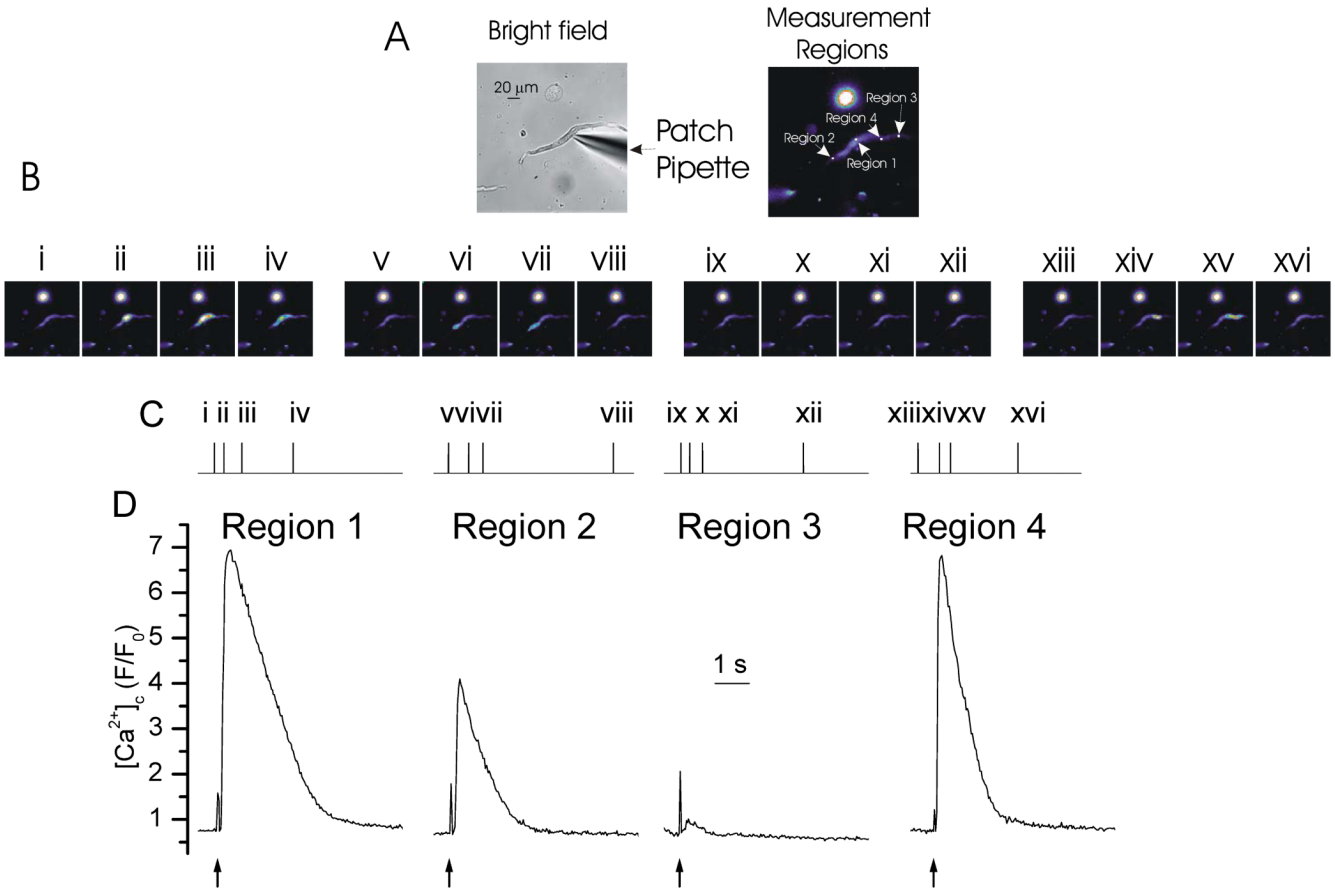

Figure 2. Various $[Ca^{2+}]_c$ increases evoked by localized photolysis of caged IP_3

IP_3 photolyzed (↑; D) at various 2 μm diameter regions in the cell (position shown in A right-hand panel) evoked increases in $[Ca^{2+}]_c$ of different amplitudes The results suggest that there are different sensitivities to IP_3 throughout the cell with the nuclear region showing higher sensitivity to IP_3 than other regions. The $[Ca^{2+}]_c$ images (B) are derived from the time points indicated by the corresponding numerals in C. $[Ca^{2+}]_c$ changes in B are represented by colour; blue low and red/white high $[Ca^{2+}]_c$. Changes in the fluorescence ratio with time (D) are derived from the boxes shown in A (right panel). (A) left panel shows a bright field image of the cell; see also whole cell electrode (right side) The spike in fluorescence on uncaging (↑) arises from the light flash used to uncage IP_3.

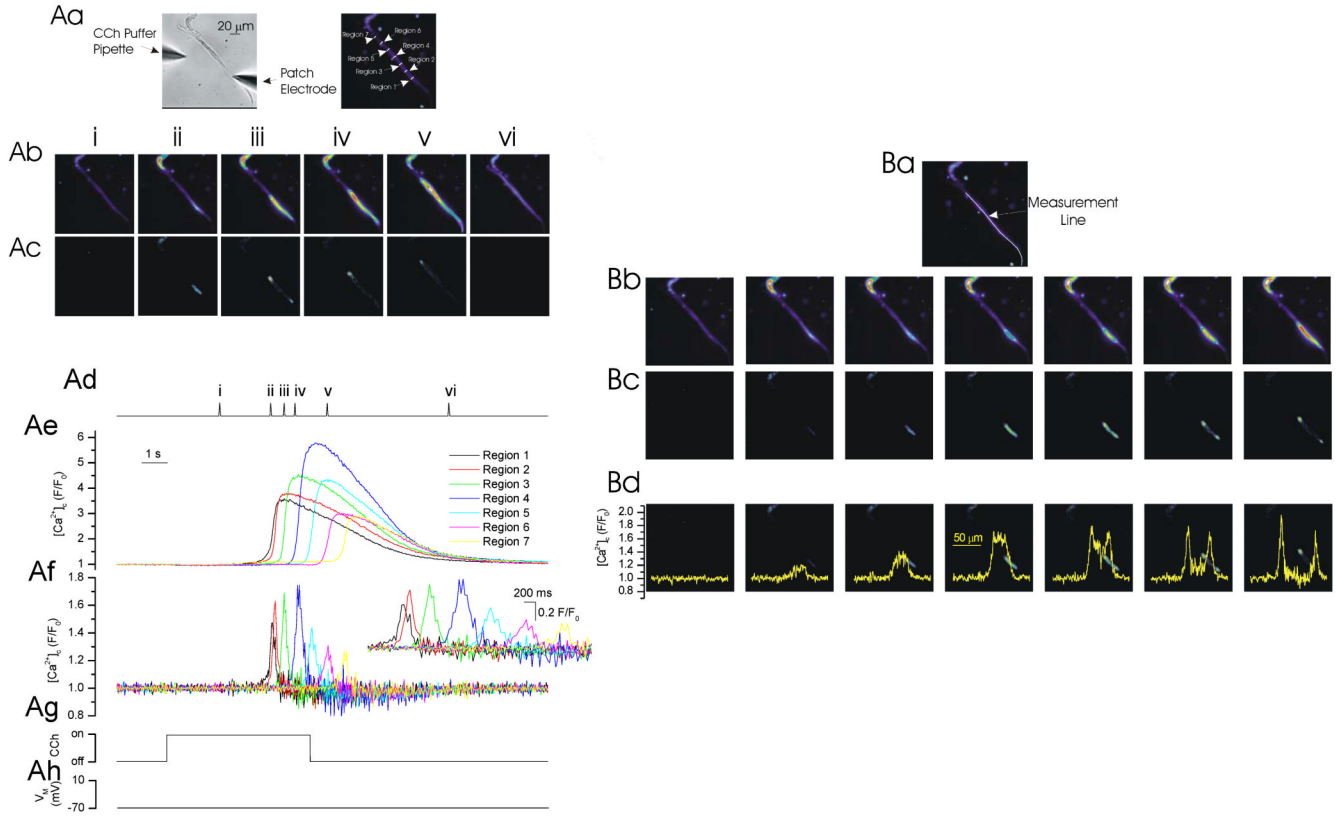

Figure 3. The CCh-evoked Ca^{2+} wave front

CCh (Ag) evoked a $[Ca^{2+}]_c$ increase which began in one part of the cell and progressed from that site (Ab, Ae). The development of the wave front is clear when the forward difference of the $[Ca^{2+}]_c$ changes is presented by sequential subtraction of the images (Ac, Af). The wave front had an approximately constant duration of ~200 ms throughout the cell (Af; inset shows the data on an expanded time base). The $[Ca^{2+}]_c$ images (Ab, Ac) are derived from the time points indicated by the corresponding numerals in Ad. $[Ca^{2+}]_c$ changes in Ab and Ac are represented by colour; blue low and red/white high $[Ca^{2+}]_c$. Changes in the fluorescence ratio with time (Ae & Af) are derived from 1 pixel lines (regions 1-7 in Aa, right panel; drawn at a 3 pixel width to facilitate visualization). (Aa) left panel shows a bright field image of the cell; see also whole cell electrode (right side) and CCh-containing puffer pipette (left side). (B) An examination of the $[Ca^{2+}]_c$ change along the length of the cell (Ba, measurement line) in sequential frames shows the wave began as a relatively uniform increase in $[Ca^{2+}]_c$ (Bc, Bd) over a substantial part of the cell (~30 μm) before progression as a wave was evident. After initiation of the wave the length of the progressing front was considerably smaller (~30%) than that which occurred at the initiation site. The frames in Bd are the same as those of Bc except with the measured $[Ca^{2+}]_c$ changes in those frames (from the line in Ba) superimposed to illustrate the nature of the developing wave front . For comparison (Bb) the wave progression is shown from the same time points. Prior to subtraction, the images were filtered using a 3x3 median filter.

Europe PMC Funders Author Manuscripts

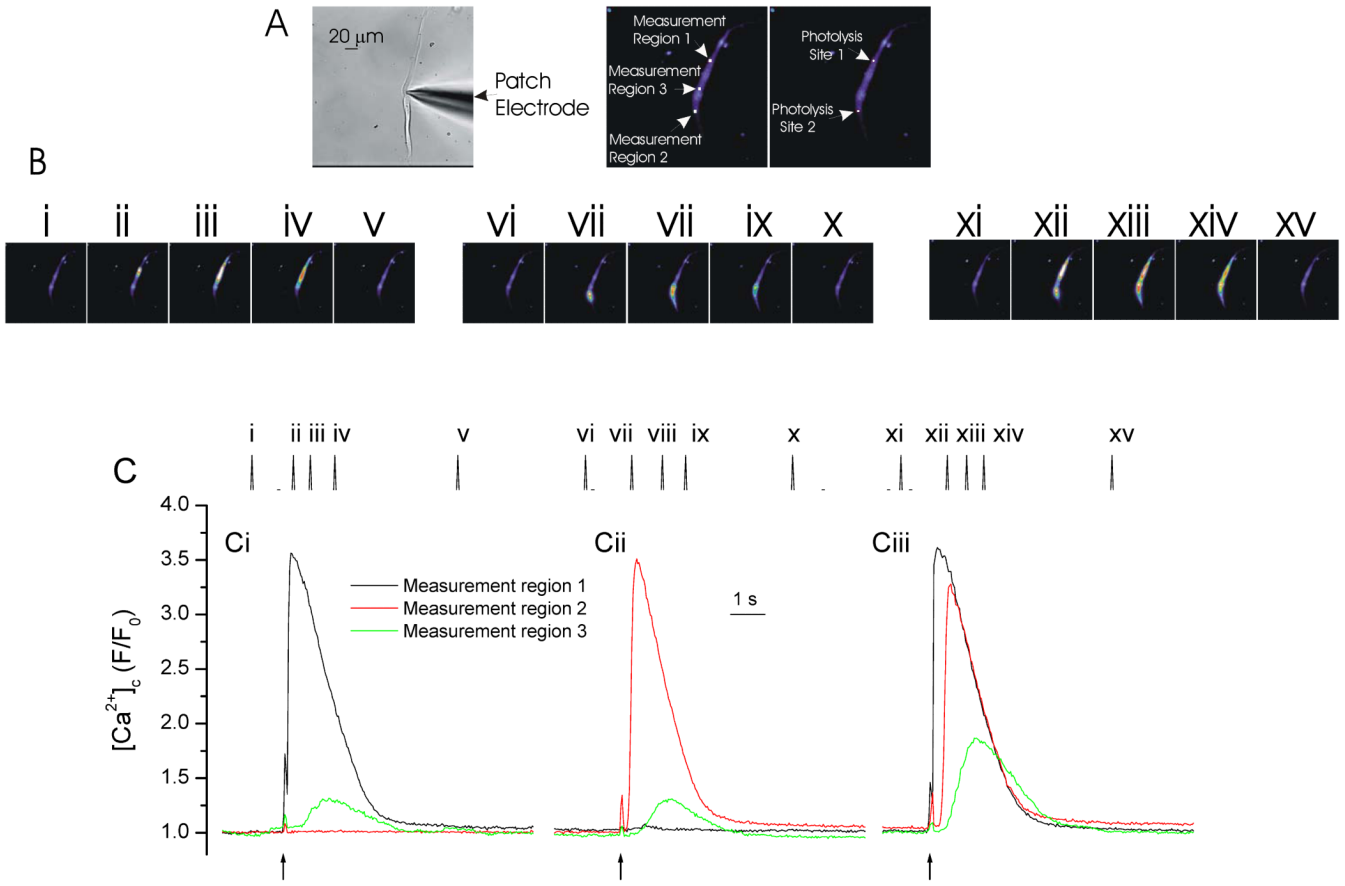

Figure 4. IP_3-evoked $[Ca^{2+}]_c$ increases

At −70 mV, locally photolyzed caged IP_3 (↑, 2 μm diameter region; position indicated by the spots in A right-hand panel) at the two peripheral regions of the cell separately (Ci & Cii) increased $[Ca^{2+}]_c$ (B,C) which was maximal at and decreased away from the release site. When IP_3 was released by photolysis at both sites almost simultaneously (2 ms apart; ↑, Ciii) the Ca^{2+} increase at the point of Ca^{2+} contact (region 3, green line) approximately doubled in amplitude. The result is consistent with the passive diffusion of Ca^{2+} from the release site. The $[Ca^{2+}]_c$ images (B) are derived from the time points indicated by the corresponding numerals in C. $[Ca^{2+}]_c$ changes in B are represented by colour; blue low and red/white high $[Ca^{2+}]_c$. Changes in the fluorescence ratio with time (C) are derived from the boxes shown in A centre panel (regions 1-3). (A) left panel shows a bright field image of the cell; see also whole cell electrode (right side). The spike in fluorescence on uncaging (↑) arises from the light flash used to uncage IP_3.

Europe PMC Funders Author Manuscripts

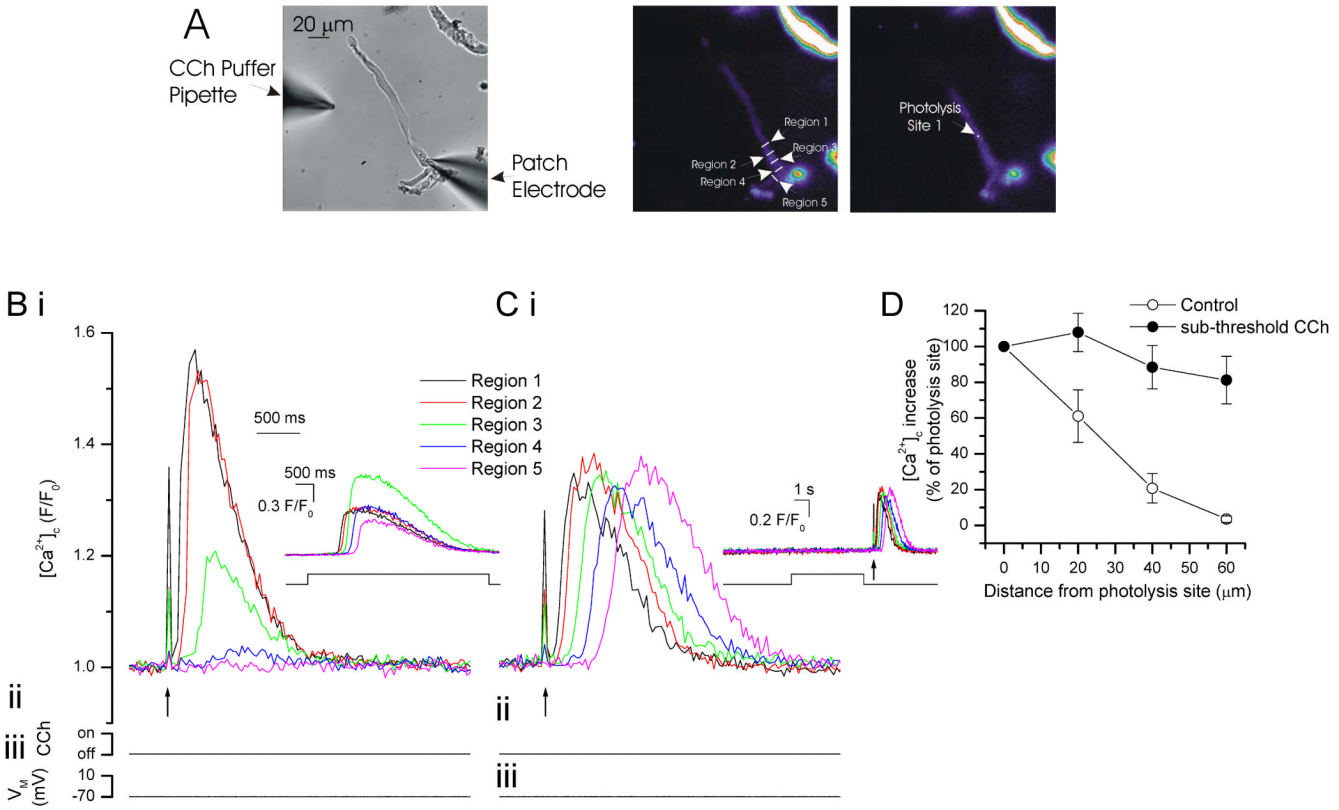

Figure 5. In the presence of sub-threshold CCh concentrations, IP_3 increased $[Ca^{2+}]_c$ and evoked waves

At −70 mV, locally photolyzed increases in IP_3 (↑, 2 μm diameter spot A, right-hand panel) increased $[Ca^{2+}]_c$ (B i). Increases were maximal at and decreased with each 10 μm step from the release site (B i; summary D (control; n=5). The region of each $[Ca^{2+}]_c$ measurement (region 1-5) corresponds to those shown in A (middle panel) where region 1 is the site of IP_3 photolysis. The inset in B shows a CCh-evoked Ca^{2+} wave in the same cell. In low concentrations of CCh (see Methods) local release of IP_3increased $[Ca^{2+}]_c$ (C i). These increases were maintained throughout the cell (C i, summary in D, n=5) i.e. they produced a propagated Ca^{2+} wave. The inset in Ci shows the sub-threshold CCh application (with no substantial Ca^{2+} change) and flash release of IP_3. The spike in fluorescence on uncaging (↑) arises from the light flash used to uncage IP_3.

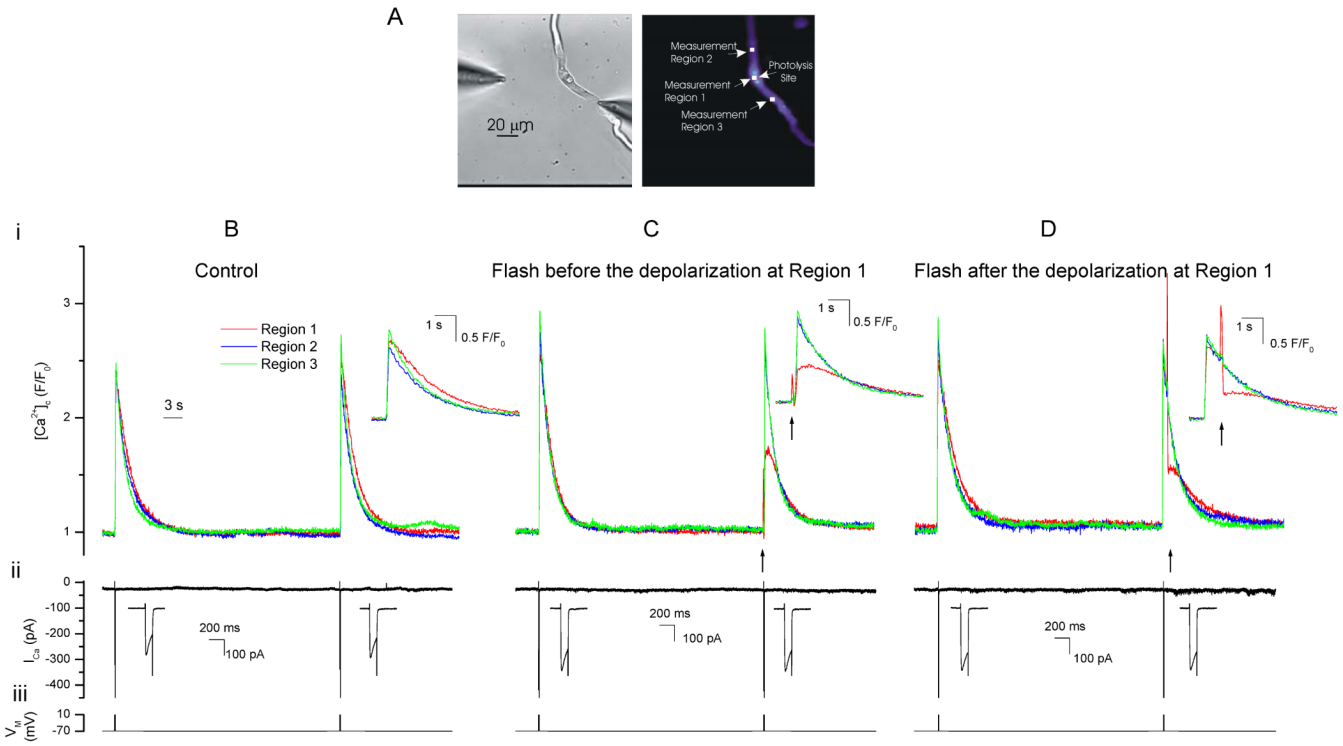

Figure 6. Photolysis of diazo-2 attenuates depolarization-evoked $[Ca^{2+}]_c$ increases

Depolarization (−70 mV to +10 mV; Biii), activated a voltage-dependent Ca^{2+} current (I_{Ca}; Bii) to evoke approximately reproducible increases in $[Ca^{2+}]_c$ when repeated at ~60 s intervals (Bi). Next the depolarization protocol (Ciii) was repeated in the same cell but, in this case, diazo-2 was photolyzed (↑) 100 ms before the second depolarization. The $[Ca^{2+}]_c$ rise (Ci) at the photolysis site (measurement region 1) was reduced by ~50% while in nearby regions the increase was unaltered. The depolarization protocol (Diii) was again repeated in the same cell but, in this case, diazo-2 was photolyzed (↑) 800 ms after the second depolarization. The $[Ca^{2+}]_c$ rise (Di) at the photolysis site (measurement region 1) was again reduced by ~50% while in nearby regions the increase was unaltered. Changes in the fluorescence ratio with time (Bi-Di) are derived from the boxes shown in A, right panel. (A) left panel shows a bright field image of the cell. Insets (Bi-Di) show the $[Ca^{2+}]_c$ transients on an expanded time base. The 'spike' in fluorescence on photolysis (Ci & Di) arises from the light flash used to uncage diazo-2. Insets (Bii-Dii) show the depolarization-evoked Ca^{2+} currents on an expanded time scale.

Europe PMC Funders Author Manuscripts

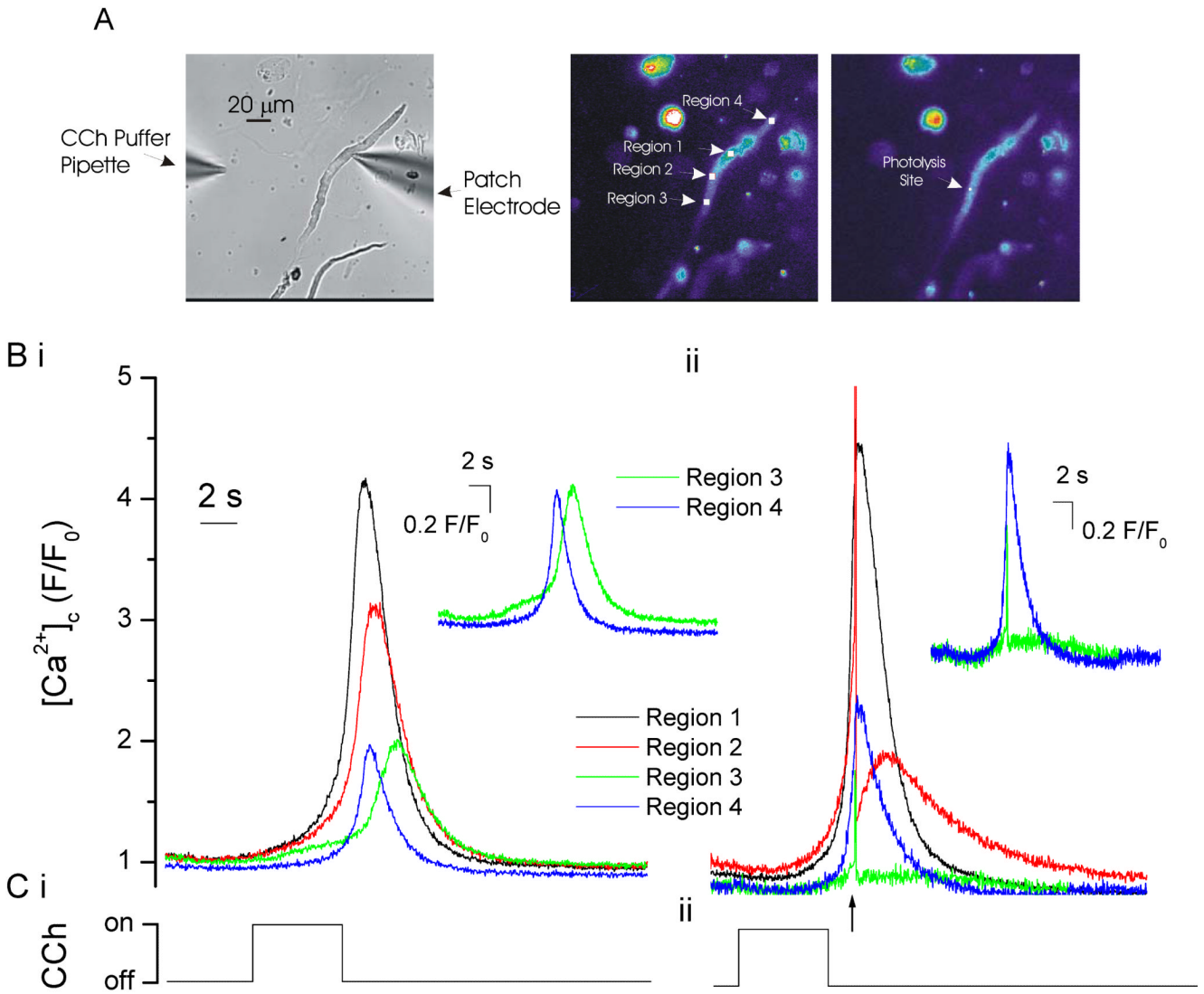

Figure 7. Ca^{2+} is required for wave progression to occur

Local photolysis of the caged Ca^{2+} buffer diazo-2 terminated wave progression. CCh (Ci) evoked a $[Ca^{2+}]_c$ increase (Bi) which began in one part of the cell (region 1; A centre panel) and progressed from that site. Next CCh (Cii) was again applied to the same cell but, in this case, diazo-2 was photolyzed (↑) just before the wave reached the photolysis site (region 2). The $[Ca^{2+}]_c$ rise (Bii) was attenuated and prolonged at the photolysis site (measurement region 2) as expected from the increased Ca^{2+} buffering at the site. Significantly, the wave did not progress beyond the site (region 3; Bii). On the other hand, at the other end of the cell (region 4), where buffering remained at control levels, the wave progressed normally. Changes in the fluorescence ratio with time (Bi & Bii) are derived from the boxes shown in A (middle panel). A, left panel shows a bright field image of the cell (see also the patch electrode and CCh-containing puffer pipette. The insets show the $[Ca^{2+}]_c$ changes in regions 3 and 4 which are of an equal distance from the site of wave origin. The spike in fluorescence on uncaging (↑) arises from the light flash used to uncage diazo-2.